



## FOXN4 affects myocardial ischemia-reperfusion injury through HIF-1 $\alpha$ /MMP2-mediated ferroptosis of cardiomyocytes

Jiyang Wang<sup>1,2</sup>, Min Deng<sup>3</sup>, Jiaona Yang<sup>4</sup>, Xiaojuan Zhou<sup>2</sup>, Peng Yang<sup>2</sup>, Yan Li<sup>5\*</sup>, Guimin Zhang<sup>1,2\*</sup>

<sup>1</sup>Department of Cardiovascular Surgery, Affiliated Cardiovascular Hospital of Kunming Medical University, Kunming, China

<sup>2</sup>Department of Cardiovascular Surgery, Affiliated Hospital of Yunnan University, Kunming, China

<sup>3</sup>Department of Anesthesiology, Affiliated Hospital of Yunnan University, Kunming, China

<sup>4</sup>Department of Medical Ultrasonics, The First Affiliated Hospital of Kunming Medical University, Kunming, China

<sup>5</sup>State Key Laboratory for Conservation and Utilization of Bio-resource in Yunnan, School of Ecology and Environmental Science, Yunnan University, Kunming, China

### ARTICLE INFO

#### Original paper

#### Article history:

Received: March 9, 2023

Accepted: June 23, 2023

Published: June 30, 2023

#### Keywords:

FOXN4, Myocardial ischemia-reperfusion injury, HIF-1 $\alpha$ , MMP2, Ferroptosis

### ABSTRACT

Myocardial ischemia-reperfusion injury (MIRI) is an important factor leading to myocardial injury and necrosis and can induce ischemic heart disease. Forkhead box protein N4 (FOXN4) belongs to the gene family of Fork head domain (Fox) transcription factors and plays an important role in heart formation and function. However, whether FOXN4 is involved in MIRI progression is unknown. In this study, we investigated the clinicopathological significance and potential mechanisms of FOXN4 in MIRI. The expressions of FOXN4 and MMP2 were measured by quantitative reverse transcriptase polymerase chain reaction, apoptosis was detected by flow cytometry and cell viability was detected by examining EdU incorporation into DNA. The signaling pathway-related proteins FOXN4, MMP2, HIF-1 $\alpha$ , apoptosis-related proteins Bcl-2 and Bax, and ferroptosis-related proteins TFR1 and IREB2 were detected by western blot, the levels of malondialdehyde (MDA), Fe<sup>2+</sup>, reactive oxygen species (ROS), and glutathione were detected by commercially available kits, and the cardiac histopathology after MIRI was evaluated by hematoxylin and eosin staining. We found that the knockdown of FOXN4 alleviated oxidative stress, inhibited ROS production, and inhibited ferroptosis in MIRI-injured tissues and cardiomyocytes. In addition, the knockdown of FOXN4 inhibited myocardial injury, improved myocardial cell viability, restored myocardial function, and alleviated MIRI. We interrogated the mechanism and found that FOXN4 can enhance its binding to HIF-1 $\alpha$ , up-regulate the expression of MMP2, and mediate ferroptosis to regulate the functional activity of cardiomyocytes to affect the progression of MIRI. This study provides new insights into the role of FOXN4 in MIRI progression and suggests that FOXN4 may represent a potential therapeutic target in MIRI progression by regulating the active function of cardiomyocytes through HIF-1 $\alpha$ /MMP2-mediated ferroptosis.

Doi: <http://dx.doi.org/10.14715/cmb/2023.69.6.33>

Copyright: © 2023 by the C.M.B. Association. All rights reserved.

### Introduction

Ischemic myocardial infarction is the leading cause of death and disability worldwide (1). Although various revascularization methods can reduce the damage caused by myocardial ischemia by timely and effectively restoring myocardial blood perfusion, the restoration of blood flow after myocardial ischemia will also be accompanied by reperfusion injury, which will further lead to myocardial cell injury or even necrosis. This phenomenon is called myocardial ischemia-reperfusion injury (MIRI) (2). The incidence of reperfusion injury can reach 50% of the total myocardial injury. At the same time, MIRI often causes serious adverse outcomes such as heart failure, arrhythmia, and even circulatory arrest (3). Potential induction mechanisms of MIRI include inflammation, disturbance of energy metabolism, oxidative stress, and apoptosis (4). In addition, the burst of ROS early in reperfusion is considered to be a major driver of the pathogenesis of MIRI (5). Therefore, it is imperative to study its pathophysiological mechanism and find effective measures to inhibit oxida-

tive stress in order to improve the prognosis of patients with coronary heart disease.

Ferroptosis is a recently described type of cell death closely related to oxidative stress, which is characterized by the generation of reactive oxygen species (ROS) and the accumulation of lipid peroxidation (6). It has been recently reported in pathological studies that ferroptosis is closely related to myocardial ischemia/reperfusion injury (7). Ferroptosis is an important form of cardiomyocyte death (8). Studies have shown that ROS plays an important role in MIRI-mediated ferroptosis. During MIRI, iron accumulates in cardiomyocytes around myocardial scars. Excess iron will lead to cardiomyocyte death, while inhibition of ROS production inhibits cardiomyocyte death (9). In addition, inhibition of ferroptosis-induced cardiomyocyte apoptosis was identified as a potentially important target in preventing cell death in general (10) and specifically in cardiac tissue (11). It was found that the ferroptosis inhibitor FER-1 and the iron chelator dexrazoxanil (DXZ) significantly up-regulated the expression level of PTGS2 mRNA in MIRI mice, reduced the myocardial infarction

\* Corresponding author. Email: G.Z. (zgm0871@163.com); Y.L. (liyan0910@ynu.edu.cn)

tion scar area, and improved MIRI-induced heart failure in mice (12). Studies have shown that overexpression of USP22 increases glutathione (GSH) levels, reduces ROS production, lipid peroxidation, and iron accumulation, and inhibits ferroptosis to alleviate MIRI. In addition, Feng et al. (13) found that Lipstatin-1 (LIP-1) inhibits iron-induced cell death, decreases the production of ROS, and elevates levels of the antioxidant protein GPX4 caused by injury/reperfusion (I/R) stress, thereby protecting the myocardium from I/R injury. These findings indicate that understanding the specific mechanism of ferroptosis and inhibiting ferroptosis-promoting cardiomyocyte death is essential to achieve effective treatment of MIRI.

Forkhead box (FOX) proteins are a family of transcription factors which are involved in a wide range of biological processes, such as embryogenesis, differentiation, transformation, and metabolic homeostasis (14). However, it is unclear whether FOXN4 is involved in MIRI by specifically regulating oxidative stress-related ferroptosis.

HIF-1 is a heterodimeric transcription factor consisting of an alpha subunit (HIF-1 $\alpha$ ) and a beta subunit (HIF-1 $\beta$ ) (15). The expression of HIF-1 $\alpha$  is induced by hypoxia and ischemia. In disease states such as cancer, ischemic heart disease, or chronic obstructive pulmonary disease, the oxygen content of tissues is reduced, leading to activation of HIF-1 $\alpha$  (16). A growing number of studies have confirmed that hypoxia-inducible factor 1- $\alpha$  (HIF-1 $\alpha$ ) plays a crucial role in controlling angiogenesis, regulating oxidative stress, and affecting proliferation and apoptosis (17). Hypoxia enhanced the expression of HIF-1 $\alpha$  and inhibited the expression of miR-10b-5p in cardiomyocytes, resulting in increased expression of PTEN, which ultimately led to massive cardiomyocyte apoptosis and impaired cardiac function after myocardial infarction (18). In addition, insulin-like growth factor binding protein-1 (IGFBP-1) alleviated acute myocardial infarction by reducing HIF-1 $\alpha$  expression and inhibiting hypoxia-induced cardiomyocyte apoptosis (19). Therefore, it is important to explore HIF-1 $\alpha$ -related signaling pathways in the regulation of myocardial ischemia-reperfusion injury.

Matrix metalloproteinase-2 (MMP2) plays an important role in cell differentiation, proliferation, apoptosis, and angiogenesis (20). MMP2 was the first of the MMP protease family reported to play a key intracellular role during oxidative stress-induced injury, and cleaves several sarcomere proteins within cardiac myocytes to affect cardiac ischemia-reperfusion injury (21). Studies have shown that MMP2 is activated by oxidative stress in cardiomyocytes after myocardial ischemia (MI), resulting in a significant increase in MMP2-containing water in plasma and the interior of the infarct (22). Likewise, proinflammatory cytokines enhance the biosynthesis of peroxynitrite in the myocardium, thereby activating intracellular MMP2 (23). Inhibition of MMP activity reduces oxidative stress-induced cardiac contractile dysfunction and prevents cleavage of several sarcomeric proteins (24). These reports suggest that MMP2 is a key regulator of cardiac remodeling. Recently, several studies have shown that the HIF-1 $\alpha$ /vascular endothelial growth factor (VEGF) signaling pathway is associated with MMP2 expression (25, 26). IH can promote the formation and development of aortic dissection (AD) through a ROS-HIF-1 $\alpha$ -MMPs-dependent pathway (27). However, whether HIF-1 $\alpha$  regulates the expression of MMP2 after MIRI and its role in the biological

function of cardiomyocytes and the progression of MIRI still need to be further explored.

In this study, we explored the function of FOXN4 in MIRI and whether FOXN4 affects MIRI progression by mediating cardiomyocyte ferroptosis through the HIF-1 $\alpha$ /MMP2 pathway.

## Materials and Methods

### Animal model

Fifty-four C57BL/6 mice were obtained from the Clinical College of Yunnan Medical University, weighed, coded and randomly assigned to the experimental groups. An MI/RI model was established, as reported previously (28). Mice were first anesthetized by intraperitoneal injection of 1% sodium pentobarbital (60 mg/kg), and then mechanically ventilated by an animal ventilator after tracheal intubation. A three-lead electrocardiogram was used to monitor the heartbeat as well as the typical electrocardiographic changes at the onset of myocardial ischemia. A microcatheter (Taimeng Technologies, Chengdu, China) was inserted into the left ventricle through the right carotid artery to assess cardiac function during the procedure. Myocardial ischemia was induced by ligation of the left anterior descending coronary artery for 30 min. Myocardial reperfusion was then performed for 4 h. The sham group was not processed. Observation of white color of the left ventricular apex and anterior wall indicated successful model induction. Recovery and redness of the left ventricular apex and anterior wall indicated successful reperfusion.

### Cell culture

H9C2 cardiomyocytes obtained from Huatuo Biotechnology Co., Ltd. were put into the culture medium (Dulbecco's Modified Eagle Medium (DMEM); Gibco BRL (Gaithersburg, MD, USA) with 10% fetal bovine serum (FBS) (Invitrogen, Waltham, MA, USA), in 5% CO<sub>2</sub> and the incubator temperature was kept at 37°C. Following a previously established protocol (29), cardiomyocytes were cultured in a hypoxic gas mixture supplemented with 95% N<sub>2</sub> and 5% CO<sub>2</sub> to induce a hypoxia/reoxygenation (H/R) injury model. The culture medium was placed in a hypoxic incubator (95% N<sub>2</sub>, 5% CO<sub>2</sub>) for 3 hours, followed by an oxygenated incubator (95% O<sub>2</sub>, 5% CO<sub>2</sub>) for another 3 hours. Control cells were incubated with 5% CO<sub>2</sub> for 6 hours at 37 °C. FOXN4 knockdown was achieved by using a lentivirus carrying a relative shRNA sequence (Sigma-Aldrich, St. Louis, MO, USA).

### Quantification of MDA, Fe<sup>2+</sup>, ROS, and GSH

Assessing the levels of MDA, Fe<sup>2+</sup>, ROS, and GSH was performed using the Lipid Peroxidation MDA Kit (Solarbio, China), the Iron Assay Kit (Solarbio, China), the ROS Assay Kit (Solarbio, China), and the GSH Assay Kits (Solarbio, China), respectively, according to the manufacturer's instructions. The levels of MDA, Fe<sup>2+</sup>, ROS, and GSH in cell supernatants and tissues were measured using a microplate reader at absorption wavelengths of 532, 593, 490, and 412 nm.

### Creatine Kinase activity assay

Creatine Kinase (CK) activity was measured using a CK test kit (Solarbio, China). Optical density (OD) values

**Table 1.** Primer sequences.

Genes	Forward (5'-3')	Reverse (5'-3')
MMP2	GAGATACAATGAGGTGAAGAAG	GACGGCATCCAGGTTATC
FOXN4	ACCTGTCTCTGAACAAGTG	GCATCTCCTCCTCCATCT
GAPDH	TGACCACAGTCCATGCCATCAC	CGCCTGCTTCACCACCTTCTTG

were measured at 660 nm with a microplate reader and a 1 cm light path according to the manufacturer's instructions. CK activity (U/mL) =  $(7.4491 \times (\text{experimental OD value} - \text{control OD value}) - 0.0716) \times \text{sample dilution time}$ .

### Determination of Cell Viability

Cell viability was measured using the CCK-8 kit (Solarbio, China) according to the manufacturer's instructions. In short, chondrocytes were seeded in 96-well plates (8,000 cells/well) and incubated with 10% FBS in DMEM/F12 for 24 hours at 37°C. Then, 10  $\mu$ L of CCK-8 solution was added to each well and cell were incubated with the solution for 4 hours. Absorbance was measured at 450 nm using a photometer (BioTek uQuant, Winooski, VT, USA).

### Mitochondrial membrane potential assay

Cardiomyocytes were incubated with JC-1 solution at 37°C for 20 minutes, washed twice with JC-1 buffer, and then media was added to each well. Images were collected using a fluorescence microscope, which detects J aggregates (excitation/emission = 525/590 nm) and JC-1 monomers (excitation/emission = 490/530 nm).

### Hematoxylin and eosin staining

Mouse heart tissue was fixed in 4% paraformaldehyde for 24 hours. Samples were then embedded in paraffin, cut into 4  $\mu$ m-thick sections, and stained using the hematoxylin-eosin staining method according to the protocol. Histopathological changes were observed under a microscope. Histopathological diagnosis was made by a pathologist through a double-blind histopathological assessment.

### TUNEL staining

Tissues were fixed in 4% phosphate-buffered neutral formalin (Beijing Solarbio Technology Co., Ltd., Beijing, China) for 20 minutes at room temperature, embedded in paraffin, cut into 5  $\mu$ m-thick sections, and then deparaffinized at room temperature followed by a drop alcohol series. The sections were subsequently incubated with 0.3% hydrogen peroxide/phosphate-buffered saline for 30 minutes. Cell death was determined using the TUNEL Apoptosis Assay Kit (Beijing Solarbio Technology Co., Ltd.) according to the manufacturer's instructions. Stained cells were counted using a light microscope (magnification, 40 $\times$ ; Olympus CK40; Olympus Life Science, Tokyo, Japan).

### Gene expression analysis

Total RNA was extracted from H9C2 cells using TRIzol reagent (Invitrogen) and then reverse transcribed into cDNA using the Prime Script<sup>TM</sup> RT kit (TaKaRa, Japan). Specific cDNA was generated using the Mir-X<sup>TM</sup> First Strand Synthesis kit (TaKaRa, Japan). Quantitative reverse transcription polymerase chain reaction (qRT-PCR) was performed using SYBR Premix Ex Taq<sup>TM</sup> II (TaKaRa, Japan). Primer sequences are shown in Table 1.

### Western blot analysis

After centrifugation and lysis of H9C2 cells and tissues, the total proteins were separated and protein concentration was determined. Protein concentration assays were performed using a BCA kit (Sigma-Aldrich). Proteins were separated on a 10% sodium dodecyl-sulfate polyacrylamide gel electrophoresis (SDS-PAGE) gel and transferred to polyvinylidene fluoride (PVDF) membrane, which was then incubated with primary antibodies against FOXN4 (1:1,000, ab287438), Bcl-2 (1:1,000, ab32124), Bax (1:1,000, ab32503), MMP2 (1:1000, ab92536), HIF-1 $\alpha$  (1:1,000, ab179483), TFR1 (1:1,000, ab214039), IREB2 (1:1,000, ab181153), and GAPDH (1:10,000, ab181602) (Abcam, Cambridge, UK) were incubated overnight at 4 °C. The secondary antibody was then incubated with the membrane for 1 hour at room temperature before the protein bands were visualized using an ECL kit. Image J software was used to quantify the densitometry and calculate the relative protein expressions.

### Statistical analysis

GraphPad Prism 8 (GraphPad Software, San Jose, CA, USA) was used for statistical analysis. Each experiment was performed at least three times. Data are expressed as mean  $\pm$  standard deviation (SD). The Student's t-test (two-tailed) was used to evaluate the differences between the two groups. Analysis of variance (ANOVA) with Tukey's post hoc test was used to evaluate differences among more than two groups. Values of  $P < 0.05$  were considered to be a statistically significant difference.

### Results

#### Knockdown of FOXN4 Attenuates MIRI Damage

FOXN4 is involved in the regulation of numerous biological functions and plays an important role in cardiovascular diseases (30). We found that the expression of FOXN4 was significantly up-regulated in the MIRI group compared to the control group at both the mRNA and protein levels, and the knockdown of FOXN4 markedly reduced the expression of FOXN4 (Figure 1A–B). In addition, we found that, compared with the control group, in the MIRI group showed abnormal induction of oxidative stress and a large accumulation of ROS (Figure 1C), which correlated with increased cardiomyocyte apoptosis (Figure 1D) and reduced cell proliferation (Figure 1E). However, these trends were reversed after the knockdown of FOXN4. Our experimental results also showed that the contents of Lactate dehydrogenase acid kinase (LDH) and creatine kinase (CK) were significantly increased in the MIRI group compared with the control group (Figure 1F), and at the same time, cardiomyocyte depolarization occurred, the resting state of membrane potential was changed to a greater extent (Figure 1G). Notably, these trends were also suppressed in the knockdown FOXN4-treated group. These results suggest that knockdown of FOXN4 attenuates MIRI.

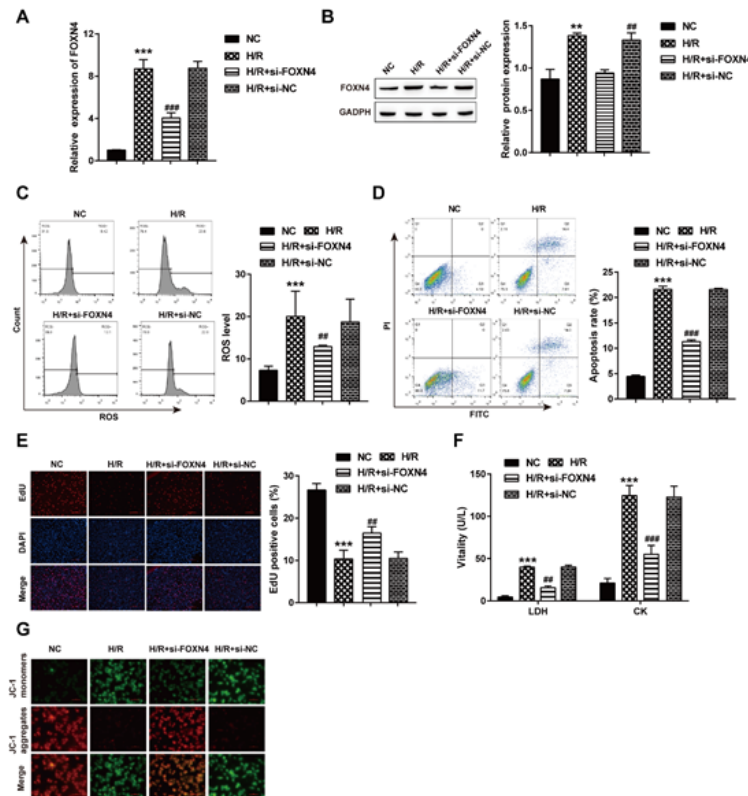


**Figure 1.** Knockdown of FOXN4 mitigates MIRI damage. (A) RT-PCR was used to detect the expression of FOXN4. (B) The expression of FOXN4 was detected by Western blot. (C) The level of ROS after oxidative stress was detected by flow cytometry. (D) Apoptosis was detected by flow cytometry. (E) Cell proliferation was measured by EdU incorporation. (F) The kit was used to detect Lactate dehydrogenase acid (LDH) and creatine kinase (CK) levels. (G) JC-1 was used to detect membrane potential. (vs NC, \*P<0.05, \*\*P<0.01, \*\*\*P<0.001; vs H/R, #P<0.05, ##P<0.01, ###P<0.001.)

### Knockdown of FOXN4 protects cardiomyocytes by inhibiting ferroptosis after MIRI

Ferroptosis is an important form of cardiomyocyte death (31). Knockdown of FOXN4 has a protective effect on cardiomyocytes, but it is not clear whether the protective effect is caused by ferroptosis induced by MIRI on cardiomyocytes. We found that after MIRI, knockdown FOXN4 inhibited oxidative stress, decreased MDA (Figure 2A), increased GSH (Figure 2B), and reduced ROS accumulation (Figure 2C). In addition, knockdown FOXN4 also reduced the accumulation of MIRI-induced Fe<sup>2+</sup> content (Figure 2D) resulting in reduced expression of transferrin TFR1 and the iron-responsive binding element IREB2 (Figure 2F). Notably, these trends were reversed in the group treated with the ferroptosis activator Erastin. In view of this, the data suggest that knockdown FOXN4 is able to inhibit MIRI-induced oxidative stress-mediated ferroptosis. Next, we examined the effect of knockdown FOXN4 on cardiomyocytes by inhibiting MIRI-induced ferroptosis. We found that, compared with the MIRI injury group, knockdown of FOXN4 significantly promoted the expression of Bcl-2 protein, but inhibited the expression of apoptotic protein Bax (Figure 2E), inhibited the apoptosis of cardiomyocytes (Figure 2G), and increased the proliferation rate of cardiomyocytes (Figure 2H). In addition, knockdown of FOXN4 reduced LDH and CK (Figure 2I) in cell culture media, and restored mitochondrial membrane potential (Figure 2J), which alleviates MIRI injury. Importantly, these effects were reversed in the group treated with the ferroptosis activator Erastin. Taken together, these results suggest that FOXN4 knockdown exerts a protective effect on cardiomyocytes by inhibiting ferroptosis

in MIRI.

### FOXN4 regulates MIRI through the downstream molecule HIF-1α

We performed co-immunoprecipitation and western blot analyses and found that FOXN4 binds to the downstream factor HIF-1α after MIRI (Figure 3A). Next, we explored the effects of MIRI and the knockdown of FOXN4 on HIF-1α. The results show that after MIRI, the knockdown of FOXN4 alleviated oxidative stress, reduced the level of ROS in cells (Figure 3B–C), and promoted the proliferation of cardiomyocytes (Figure 3D). We examined the levels of proteins involved in apoptosis and found that Bcl-2 protein expression was promoted, but Bax protein expression was inhibited in cardiomyocytes after MIRI with knockdown of FOXN4 (Figure 3E–F), indicating that disrupting FOXN4 inhibits apoptosis. Concurrently, we observed an increase in HIF-1α levels (Figure 3E–F). In addition, knockdown of FOXN4 reduced LDH (Figure 3G) and CK (Figure 3H) levels in cell culture media, and restored mitochondrial membrane potential (Figure 3I), alleviating the effects caused by MIRI. Notably, these outcomes were reversed by overexpression of HIF-1α (Figure 3B–I). These results suggest that knockdown of FOXN4 promotes cardiomyocyte proliferation, inhibits apoptosis, and protects against MIRI by inhibiting the expression of HIF-1α.

### The protective effect of FOXN4 knockdown on MIRI can be achieved by inhibiting the HIF-1α/MMP2 signaling pathway

We further investigated the effect of knockdown

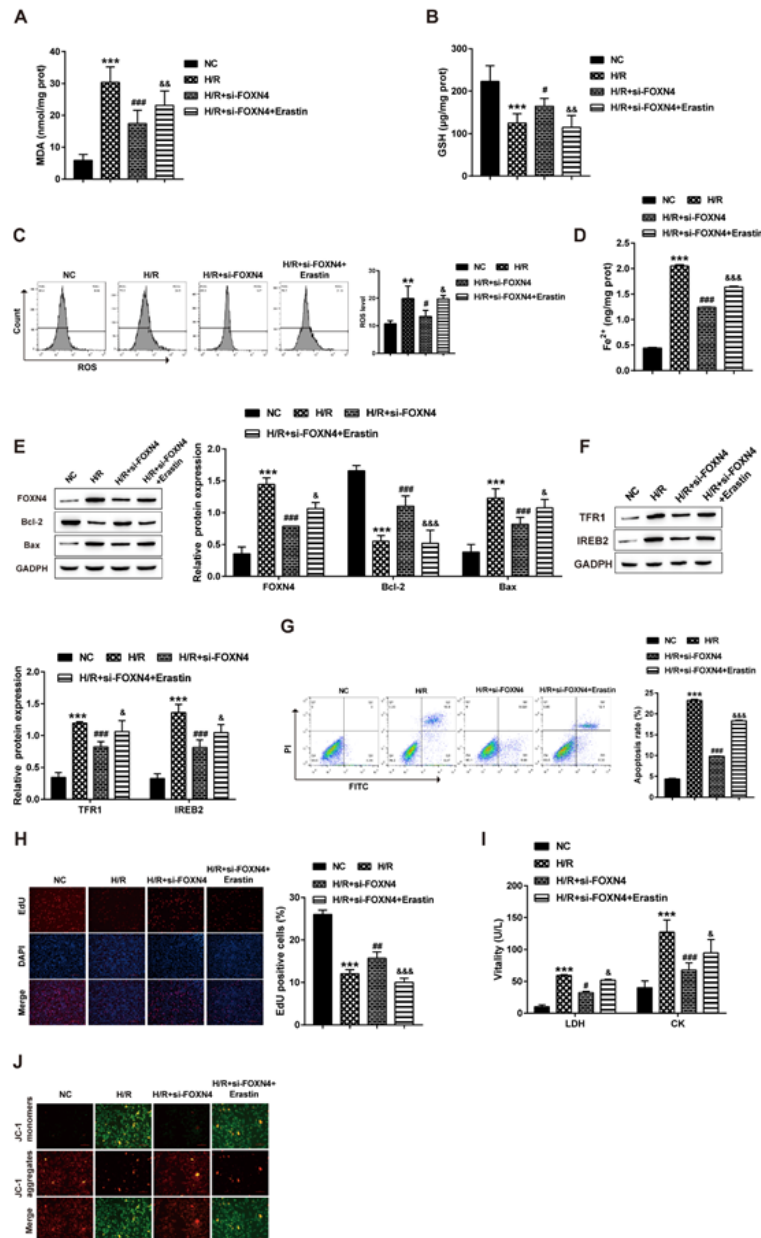


**Figure 2.** Knockdown of FOXN4 exerts a protective effect on cardiomyocytes by inhibiting ferroptosis in MIRI. (A) Kit was used to detect the content of MDA. B: The content of GSH was detected by Elisa Kit. (C) The level of ROS was measured by flow cytometry. (D) Kit to detect the content of Fe<sup>2+</sup>. (E-F) The expressions of FOXN4, Bcl-2, Bax, TFR1 and IREB2 were detected by Western blotting. (G) Flow cytometry tests for cell apoptosis. (H) Cell proliferation was detected by EDU. (I) Kit for detection of LDH and CK. (J) The membrane potential was measured by JC-1. (vs NC, \*P<0.05, \*\*P<0.01, \*\*\*P<0.001; vs H/R, #P<0.05, ##P<0.01, ###P<0.001; vs H/R+si-FOXN4, &P<0.05, &&P<0.01, &&&P<0.001).

FOXN4 on the downstream molecular mechanism MIRI mediated by HIF-1 $\alpha$ . Activated MMP2 has been reported to affect cardiac IR injury by cleaving cardiac troponin I and promoting the expression of cardiomyocyte apoptosis-related proteins (32). However, whether knockdown FOXN4 is able to affect HIF-1 $\alpha$  to inhibit MMP2 expression in MIRI remains unclear. We performed RT-qPCR and western blot analyses and found that knockdown of FOXN4 significantly reduced the expression of MMP2 after MIRI and was reversed by treatment with the MMP2 activator  $\beta$ -Neo-Endorphin (Figure 4A). Next, we investigated the effect of FOXN4 knockdown on the functional activity of cardiomyocytes through the HIF-1 $\alpha$ /MMP2 axis. Our results show that, compared with the MIRI injury group, knockdown of FOXN4 inhibited oxidative stress, reduced the accumulation of ROS (Figure 4B), inhibited cardiomyocyte apoptosis (Figure 4C–D), promoted the

expression of Bcl-2 protein, and inhibited the expressions of Bax and HIF-1 $\alpha$  proteins (Figure 4E). Additionally, knockdown of FOXN4 reduced LDH (Figure 4F) and CK (Figure 4G) in cell culture media, and restored mitochondrial membrane potential (Figure 4H), reducing the effects of MIRI. These trends were reversed by treatment with the MMP2 activator  $\beta$ -Neo-Endorphin. These results suggest that the knockdown of FOXN4 protects against MIRI by inhibiting the HIF-1 $\alpha$ /MMP2 axis to restore myocardial function.

### Knockdown of FOXN4 Attenuates Myocardial Ischemia-reperfusion in Mice via HIF-1 $\alpha$ /MMP2 Signaling Pathway

We next investigated the role of FOXN4 in MIRI via the HIF-1 $\alpha$ /MMP2 signaling pathway in mice. We found that the knockdown of FOXN4 significantly improved

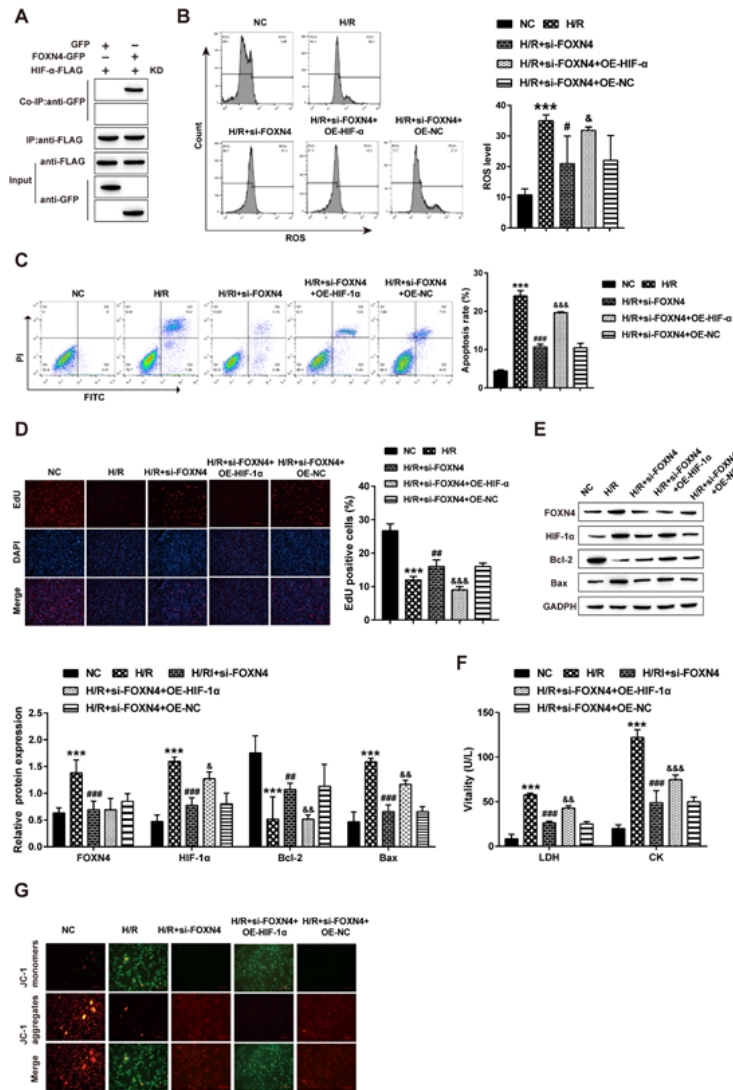


**Figure 3.** FOXN4 regulates MIRI by mediating downstream molecule HIF-1 $\alpha$ . (A) Co-immunoprecipitation and western blot analysis of that relationship between FOXN4 and HIF-1 $\alpha$ . (B–C) The levels of ROS (B) and apoptosis (C) were detected by flow cytometry. (D) Cell proliferation was detected by EdU incorporation. (E) The expressions of FOXN4, HIF-1 $\alpha$ , Bcl-2, and Bax were detected by Western blot. (F) Levels of lactate dehydrogenase (LDH) and creatine kinase (CK) in cell culture media were detected using commercially available kits. (G) Mitochondrial membrane potential was measured by JC-1 staining. vs NC, \* $P < 0.05$ , \*\* $P < 0.01$ , \*\*\* $P < 0.001$ ; vs H/R, # $P < 0.05$ , ## $P < 0.01$ , ### $P < 0.001$ ; vs H/R+si-FOXN4, & $P < 0.05$ , && $P < 0.01$ , &&& $P < 0.001$ .

the disordered arrangement of myocardial fibers and the massive deposition of collagen after MIRI (Figure 5A). Concurrently, the knockdown of FOXN4 reduced lactate LDH and CK (Figure 5B) in serum, and significantly reduced the tissue lesion volume of MIRI (Figure 5C), alleviating the effects of MIRI. However, these trends were reversed after treatment with  $\beta$ -neo-Endorphin. In addition, western blotting results show that knockdown of FOXN4 reduced the protein levels of FOXN4, HIF-1 $\alpha$ , and MMP2 (Figure 5F), inhibited oxidative stress, reduced the level of ROS (Figure 5D), inhibited apoptosis (Figure 5E), promoted the expression of Bcl-2 protein, and inhibited the expression of Bax protein (Figure 5G). Consistent with our results to this point, these trends were reversed in the  $\beta$ -neo-Endorphin treated group. These results indicate that knockdown of FOXN4 alleviates the effects of MIRI in mice by inhibiting the HIF-1 $\alpha$ /MMP2 signaling pathway.

### Knockdown of FOXN4 inhibits myocardial ischemia-reperfusion-induced ferroptosis in mice via the HIF-1 $\alpha$ /MMP2 signaling pathway

Next, we investigated the effect of FOXN4 on MIRI in

vivo through the HIF-1 $\alpha$ /MMP2 signaling pathway by modulating ferroptosis. Knockdown of FOXN4 significantly improved the disorganized arrangement of myocardial fibers and the massive deposition of collagen after MIRI (Figure 6A). Knockdown of FOXN4 also reduced levels of LDH and CK (Figure 6B) in serum, and reduced the tissue lesion volume of MIRI (Figure 6C), alleviating MIRI. In agreement with our results to this point, these trends were blocked by treatment with the MMP2 inhibitor Pyridoxatin treated group, and this effect was reversed by treatment with the ferroptosis activator Erastin. In addition, the knockdown of FOXN4 inhibited the expressions of proteins FOXN4, HIF-1 $\alpha$ , and MMP2 (Figure 6H), inhibited oxidative stress, decreased MDA levels (Figure 6D), and reduced ROS accumulation (Figure 6E). Knockdown of FOXN4 also reduced MIRI-induced ferroptosis, reduced the accumulation of Fe<sup>2+</sup> content (Figure 6F), and down-regulated the expression of transferrin TFR1 and iron-responsive binding element IREB2 (Figure 6I). Additionally, FOXN4 knockdown inhibited cardiomyocyte apoptosis (Figure 6G), promoted Bcl-2 protein expression, and inhibited Bax protein expression (Figure 6H). Consistent with

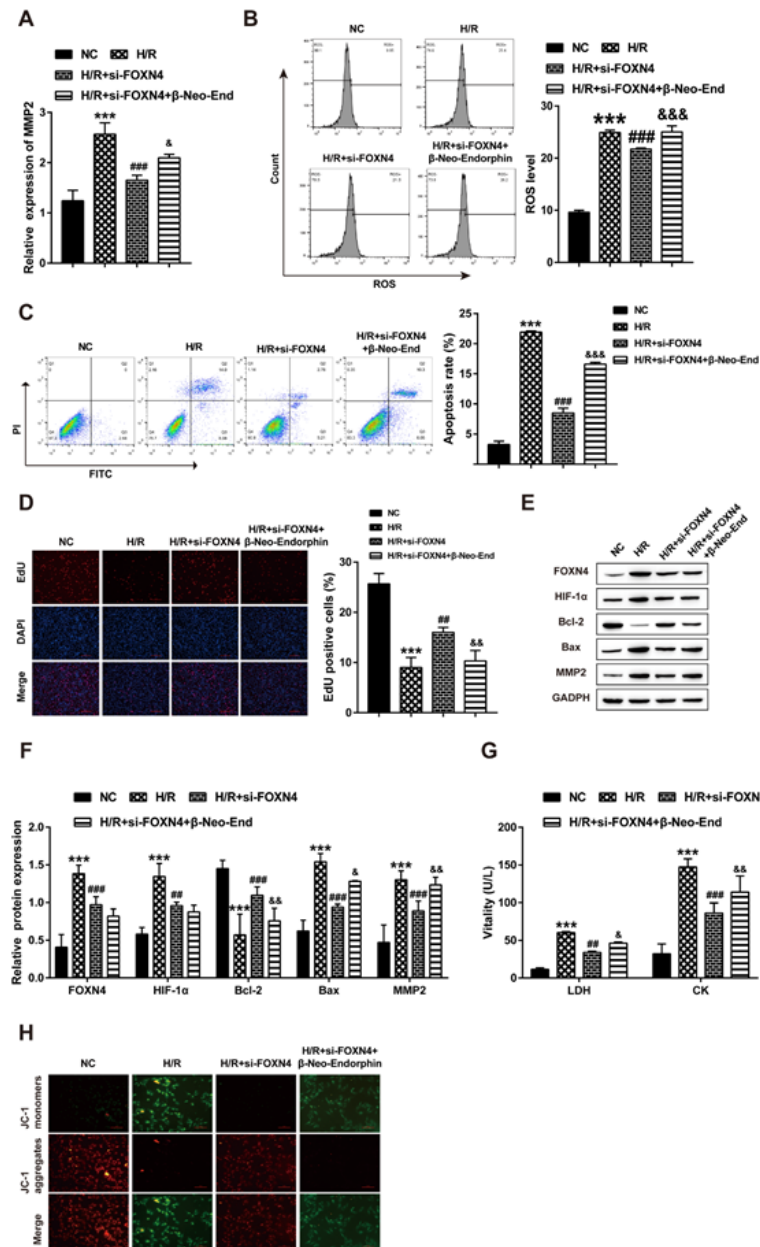


**Figure 4.** The protective effect of FOXN4 knockdown on MIRI was achieved by inhibiting the HIF-1 $\alpha$ /MMP2 signaling pathway. (A) RT-PCR was used to quantify the expression of MMP2. (B–C) The levels of ROS (B) and apoptosis (C) were detected through flow cytometry. (D) Cell proliferation was detected by EdU incorporation. (E–F) The expressions of FOXN4, HIF-1 $\alpha$ , MMP2, Bcl-2, and Bax were detected by western blot. (G) Levels of lactate dehydrogenase (LDH) and creatine kinase (CK) in cell culture media were detected using commercially available kits. (H) JC-1 staining was used to detect mitochondrial membrane potential. vs NC, \*P<0.05, \*\*P<0.01, \*\*\*P<0.001; vs H/R, #P<0.05, ##P<0.01, ###P<0.001; vs H/R+si-FOXN4, &P<0.05, &&P<0.01, &&&P<0.001.

our *in vitro* results, these trends were blocked by treatment with **Pyridoxatin**, and this was reversed by treatment with the ferroptosis activator Erastin. These experimental results suggest that FOXN4 knockdown may inhibit myocardial ischemia-reperfusion-induced ferroptosis and alleviate MIRI in mice through the HIF-1 $\alpha$ /MMP2 signaling pathway.

### Discussion

MIRI is one of the major fatal diseases in the world, which can induce myocardial necrosis, cardiac insufficiency, myocardial infarction, and heart failure (33). FOXN4 belongs to the N family of forkhead transcription factors and is involved in a wide variety of biological processes, especially in cell differentiation (34). Previous studies have shown that targeted disruption of FOXN4 results

in the loss of most amacrin and all horizontal cells and reduces progenitor proliferation (35). This study aims to investigate the function of FOXN4 in MIRI and elucidate the underlying molecular regulatory mechanisms. The results indicate that FOXN4 plays an important role in the induction of myocardial ischemia-reperfusion *in vivo* and *in vitro*. First, we observed high expression of FOXN4 in MIRI, and we subsequently explored the effect of FOXN4 on cardiomyocytes in a mouse model of myocardial injury. Through LDH, TTC, staining and TUNEL staining, we found that compared with the injury group alone, the FOXN4 knockdown group showed significantly enhanced viability and reduced apoptosis of cardiomyocytes. CK levels were low in the injured group, and disruption of FOXN4 increased CK levels and significantly restored myocardial function. In addition, tissue staining results showed that a large number of cardiomyocytes were necro-

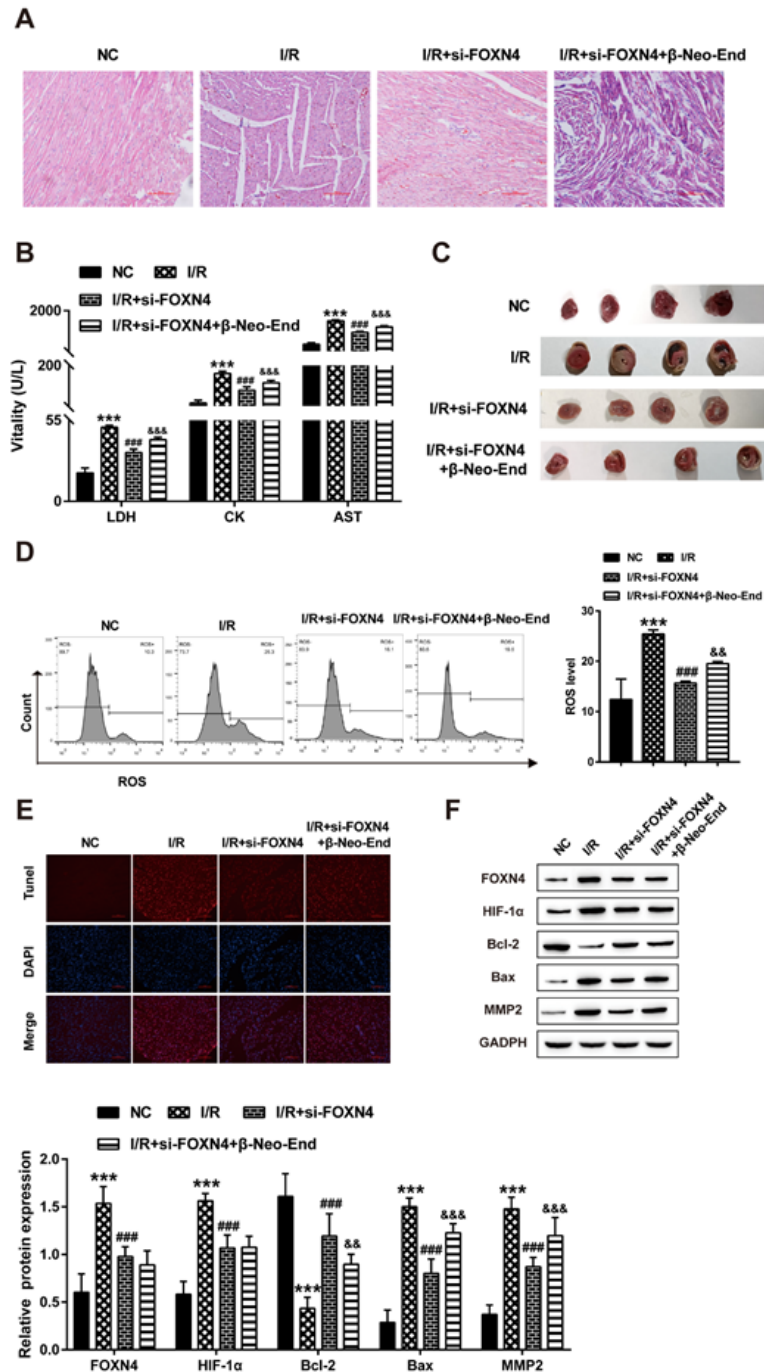


**Figure 5.** Knockdown of FOXN4 alleviates myocardial ischemia-reperfusion in mice via HIF-1 $\alpha$ /MMP2 signaling pathway. (A) H&E staining was performed to examine MIRI injury in mice. (B) Levels of lactate dehydrogenase (LDH) and creatine kinase (CK) in serum were detected using commercially available kits. (C) Images of hearts to assess MIRI size. (D) ROS was detected by flow cytometry. (E) Apoptosis was detected by TUNEL (F) The expressions of FOXN4, HIF-1 $\alpha$ , MMP2, Bcl-2, and Bax were detected by western blot. vs NC, \*P<0.05, \*\*P<0.01, \*\*\*P<0.001; vs I/R, #P<0.05, ##P<0.01, ###P<0.001; vs I/R+si-FOXN4, &P<0.05, &&P<0.01, &&&P<0.001.

tic after MIRI, which was reversed by FOXN4 knockdown to restore myocardial function, promote cardiomyocyte proliferation, and alleviate MIRI. Thus, our data suggest that the contribution of FOXN4 on the effects of MIRI is, at least in part, from its effect on the functional activity of cardiomyocytes.

An increasing amount of evidence has suggested that HIF1- $\alpha$  plays an important role in MIRI (34). After MIRI, the hypoxic environment induces the activation of HIF1- $\alpha$  and many protective genes, and the activated HIF1- $\alpha$  can contribute to MIRI by directly or indirectly participating in many signaling pathways. It has been shown that high expression levels of HIF1- $\alpha$  during hypoxia or ischemia can trigger a cascade of events, including apoptosis (36).

Inhibition of HIF1- $\alpha$  activity reduces I/R and H/R injury in rat heart and cardiomyocytes (37). Therefore, it is critical to understand the role of HIF1- $\alpha$  signaling pathway during MIRI. In this study, co-immunoprecipitation assays demonstrate that FOXN4 regulates cardiomyocyte biological functions by enhancing binding to HIF1- $\alpha$  under MIRI conditions. The results show that low expression of FOXN4 reduced the level of ROS, inhibited cardiomyocyte apoptosis, downregulated the expression of Bax, upregulated the expression of Bcl-2, and improved and restored the function and mitochondrial membrane potential of cardiomyocytes, which was reversed by overexpression of HIF1- $\alpha$ . Based on these data, we conclude that FOXN4 promotes MIRI by upregulating the expression of HIF1- $\alpha$ .

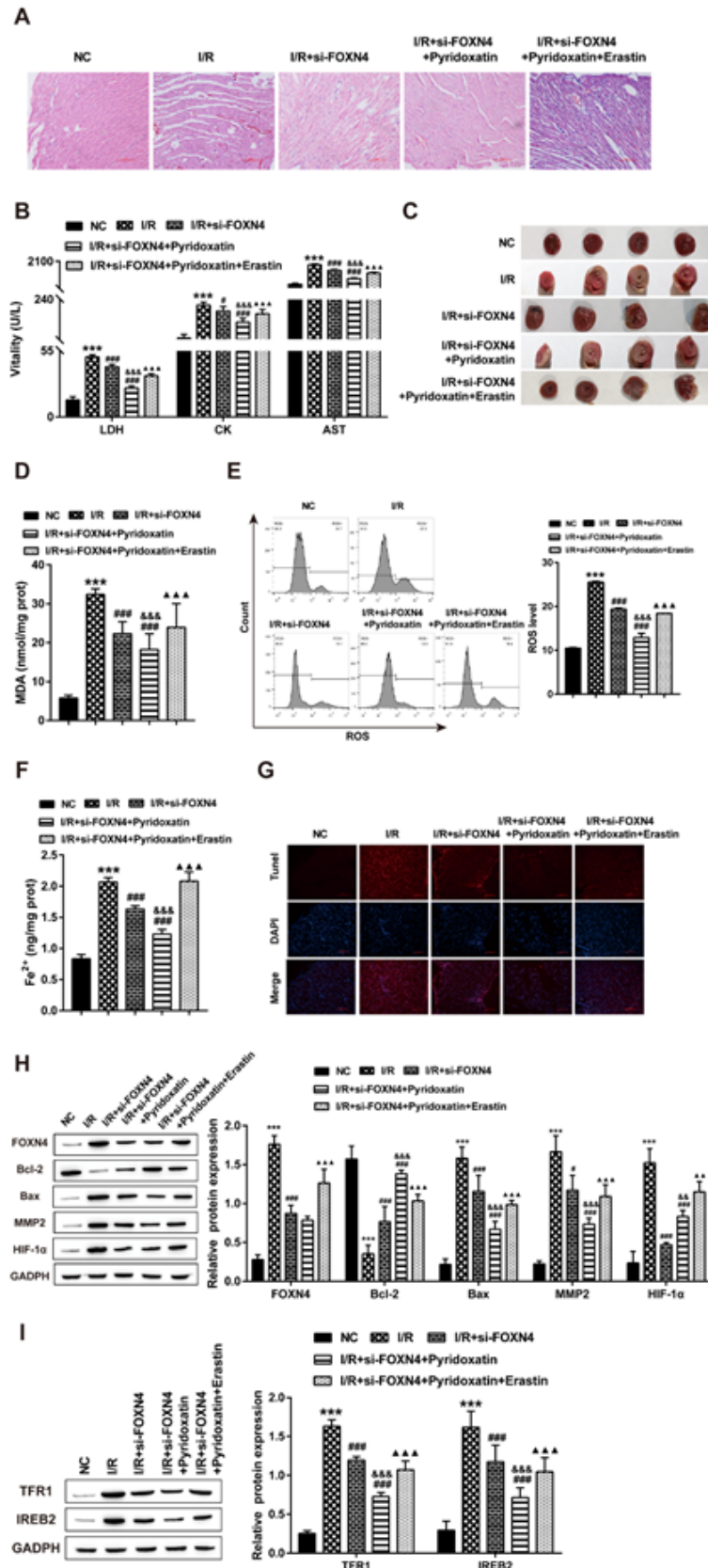


**Figure 6.** FOXN4 regulates ferroptosis induced by myocardial ischemia-reperfusion in mice through HIF-1 $\alpha$ /MMP2 signaling pathway. (A) MIRI was detected by H&E staining. (B) Lactate dehydrogenase (LDH) and creatine kinase (CK) (C) levels in serum were detected using commercially available kits. (C) Images of hearts to assess MIRI size. (D) The content of MDA was detected using a commercially available kit. (E) The level of ROS was detected by flow cytometry. (F) The content of Fe<sup>2+</sup> was detected using a commercially available kit. (G) Apoptosis was detected by TUNEL. (H-I) The expressions of FOXN4, HIF-1 $\alpha$ , MMP2, Bcl-2, Bax, TFR1, and IREB2 were detected by Western blot. vs NC, \*P<0.05, \*\*P<0.01, \*\*\*P<0.001; vs I/R, #P<0.05, ##P<0.01, ###P<0.001; vs I/R+si-FOXN4, &P<0.05, &&P<0.01, &&&P<0.001; vs I/R+si-FOXN4+Pyridoxatin, ▲P<0.05, ▲▲P<0.01, ▲▲▲P<0.001;

and promoting cardiomyocyte apoptosis.

Intracellular matrix metalloproteinases have been implicated in the pathogenesis of diverse disease condi-

tions, including cardiovascular disease (38), inflammatory conditions (39), and kidney disease (40). Studies have shown that MMP2 localizes to cardiomyocytes and affects

cardiac ischemia-reperfusion injury by cleaving cardiac troponin I (41). MMP2 induces actin cleavage in rat and human hearts during myocardial injury (42), resulting in myocardial systolic dysfunction. In addition, MMP2 protein expression level was positively correlated with Bax expression, but negatively correlated with Bcl-2 expression level, promoting apoptosis (43). Interestingly, intracellular MMP2 is also involved in the regulation of inducing or preventing ischemia-reperfusion injury by acting as a downstream target gene. In cardiomyocytes, disrupting MMP2 expression increases baseline cardiomyocyte contractility and prevents simulated ischemia-reperfusion injury (44). Similarly, in this study, we found that FOXN4 could significantly enhance MMP2 expression, promote cardiomyocyte apoptosis, and attenuate cardiomyocyte function and mitochondrial membrane potential, thereby promoting the progression of MIRI. It is worth noting that our western blotting results in this study show that the expressions of FOXN4, HIF1- $\alpha$ , and MMP2 were significantly up-regulated in the MIRI injury group, and our previous study showed that FOXN4 could enhance the binding of HIF1- $\alpha$  and regulate the biological function of cardiomyocytes involved in the process of MIRI. Therefore, we speculate that FOXN4 may play a role in MIRI by enhancing the binding of HIF1- $\alpha$  and promoting the expression of MMP2.

A growing body of research has recently linked ferroptosis to the progression of MIRI (45). Mechanistically, after MIRI, oxidative stress occurs to generate a large amount of ROS, and then the generated ROS will induce lipid peroxidation in polyunsaturated fatty acids in cells, leading to ferroptosis in cardiomyocytes (46). Li et al. (47) report that myocardial ischemia-reperfusion injury increases oxidative stress generation and causes widespread cardiomyocyte death by inducing ferroptosis. Consistent with this, we found that after MIRI injury, ROS levels rose and Fe<sup>2+</sup> and lipid oxide MDA accumulated, but GSH levels decreased. Concurrently, the Bcl-2 protein levels and the viability of cardiomyocytes decreased, while the protein levels of Bax and the apoptosis rate increased. Decreased cardiomyocyte function and mitochondrial membrane potential was similarly reversed by low expression of FOXN4. Here, we show that FOXN4 promotes the development of MIRI by inducing ferroptosis and promoting myocardial apoptosis. Interestingly, MMP2 inhibitors were found to reduce ROS levels as well as Fe<sup>2+</sup> and MDA accumulation but increase GSH levels in cardiomyocytes, but these effects were reversed by the ferroptosis activator Erastin. MMP2 inhibitors also reduced the apoptosis of cardiomyocytes and restored the function and mitochondrial membrane potential of cardiomyocytes. However, Erastin could reverse these effects. In conclusion, FOXN4 promotes the development of MIRI by inducing ferroptosis, and its intrinsic molecular mechanism may be that FOXN4 induces ferroptosis through HIF1- $\alpha$ /MMP2, affects myocardial functional activity and mitochondrial membrane potential, and promotes cardiomyocyte apoptosis, and these effects promote the development of MIRI.

Taken together, this study is identifying the effects and elucidates more of the mechanism of FOXN4-induced ferroptosis on the biological function of cardiomyocytes. The present study provides further evidence for the role of HIF1- $\alpha$ /MMP2 signaling downstream of FOXN4. However, it is unclear whether FOXN4 is involved in other

signaling pathways in MIRI. Taken together, our experiments show that FOXN4 can enhance MIRI injury by modulating the HIF1- $\alpha$ /MMP2 axis to induce ferroptosis. Our results suggest that FOXN4 may be a promising clinical predictor for the diagnosis of MIRI susceptibility and that targeting it may be a novel therapeutic strategy.

#### Author Contributions

Conceptualization, Jiyang Wang, Guimin Zhang and Yan Li; methodology, Jiyang Wang, Min Deng and Guimin Zhang; software, Jiyang Wang and Jiaona Yang; validation, Xiaojuan Zhou and Peng Yang; formal analysis, Jiyang Wang, Guimin Zhang and Yan Li; investigation, Jiyang Wang, Guimin Zhang, Yan Li and Jiaona Yang; resources, Guimin Zhang and Yan Li; writing—original draft preparation, Jiyang Wang, Guimin Zhang and Yan Li; writing—review and editing, Jiyang Wang, Guimin Zhang, Min Deng and Xiaojuan Zhou; visualization, Min Deng, Jiaona Yang and Peng Yang; supervision, Jiyang Wang, Guimin Zhang and Yan Li; funding acquisition, Guimin Zhang. All authors have read and agreed to the published version of the manuscript.

#### Funding

The present study was supported by Yunnan Province ten thousand people plan, famous doctor special (project number: 2018-001 YNWR-MY-2018-001); Basic Research Program of Science and Technology Program of Science and Technology Department of Yunnan Province, Project name: "Study on the Mechanism of Long Non-coding RNA FTX Alleviating Cardiac Injury Induced by Ischemia-Reperfusion (MI/RI)" (project number: 202101AY070001-285)

#### Availability of data and materials

The data sets used and/or analyzed during the current study are available from the corresponding author upon reasonable request.

#### Conflicts of interest

The authors declare no conflict of interest.

#### References

1. Minamino T. Cardioprotection from ischemia/reperfusion injury: basic and translational research. *Circ J* 2012; 76(5): 1074-1082.
2. Frank A, Bonney M, Bonney S, Weitzel L, Koeppen M, Eckle T. Myocardial ischemia reperfusion injury: from basic science to clinical bedside. *Semin Cardiothorac V* 2012; 16(3): 123-132.
3. Chen Z, Wu D, Li L, Chen L. Apelin/APJ System: A Novel Therapeutic Target for Myocardial Ischemia/Reperfusion Injury. *Dna Cell Biol* 2016; 35(12): 766-775.
4. Murphy E, Steenbergen C. Mechanisms underlying acute protection from cardiac ischemia-reperfusion injury. *Physiol Rev* 2008; 88(2): 581-609.
5. Cadenas S. ROS and redox signaling in myocardial ischemia-reperfusion injury and cardioprotection. *Free Radical Bio Med* 2018; 117(76-89).
6. Li J, Cao F, Yin HL, et al. Ferroptosis: past, present and future. *Cell Death Dis* 2020; 11(2): 88.
7. Park TJ, Park JH, Lee GS, et al. Quantitative proteomic analyses reveal that GPX4 downregulation during myocardial infarction contributes to ferroptosis in cardiomyocytes. *Cell Death Dis* 2019; 10(11): 835.

8. Kobayashi M, Suhara T, Baba Y, Kawasaki NK, Higa JK, Matsui T. Pathological Roles of Iron in Cardiovascular Disease. *Curr Drug Targets* 2018; 19(9): 1068-1076.
9. Baba Y, Higa JK, Shimada BK, et al. Protective effects of the mechanistic target of rapamycin against excess iron and ferroptosis in cardiomyocytes. *Am J Physiol-Heart C* 2018; 314(3): H659-H668.
10. Wu D, Chen L. Ferroptosis: a novel cell death form will be a promising therapy target for diseases. *Acta Bioch Bioph Sin* 2015; 47(10): 857-859.
11. Fang X, Wang H, Han D, et al. Ferroptosis as a target for protection against cardiomyopathy. *P Natl Acad Sci Usa* 2019; 116(7): 2672-2680.
12. Ma S, Sun L, Wu W, Wu J, Sun Z, Ren J. USP22 Protects Against Myocardial Ischemia-Reperfusion Injury via the SIRT1-p53/SLC7A11-Dependent Inhibition of Ferroptosis-Induced Cardiomyocyte Death. *Front Physiol* 2020; 11(551318).
13. Feng Y, Madungwe NB, Imam AA, Tombo N, Bopassa JC. Liproxstatin-1 protects the mouse myocardium against ischemia/reperfusion injury by decreasing VDAC1 levels and restoring GPX4 levels. *Biochem Bioph Res Co* 2019; 520(3): 606-611.
14. Yahagi K, Davis HR, Arbustini E, Virmani R. Sex differences in coronary artery disease: pathological observations. *Atherosclerosis* 2015; 239(1): 260-267.
15. Wang GL, Semenza GL. Purification and characterization of hypoxia-inducible factor 1. *J Biol Chem* 1995; 270(3): 1230-1237.
16. Masoud GN, Li W. HIF-1alpha pathway: role, regulation and intervention for cancer therapy. *Acta Pharm Sin B* 2015; 5(5): 378-389.
17. Kim SY, Yang EG. Recent Advances in Developing Inhibitors for Hypoxia-Inducible Factor Prolyl Hydroxylases and Their Therapeutic Implications. *Molecules* 2015; 20(11): 20551-20568.
18. Adamovich Y, Ladeux B, Golik M, Koeners MP, Asher G. Rhythmic Oxygen Levels Reset Circadian Clocks through HIF1alpha. *Cell Metab* 2017; 25(1): 93-101.
19. Wu L, Chen Y, Chen Y, et al. Effect of HIF-1alpha/miR-10b-5p/PTEN on Hypoxia-Induced Cardiomyocyte Apoptosis. *J Am Heart Assoc* 2019; 8(18): e11948.
20. Tang X, Jiang H, Lin P, et al. Insulin-like growth factor binding protein-1 regulates HIF-1alpha degradation to inhibit apoptosis in hypoxic cardiomyocytes. *Cell Death Discov* 2021; 7(1): 242.
21. Page-McCaw A, Ewald AJ, Werb Z. Matrix metalloproteinases and the regulation of tissue remodelling. *Nat Rev Mol Cell Bio* 2007; 8(3): 221-233.
22. Bassiouni W, Ali M, Schulz R. Multifunctional intracellular matrix metalloproteinases: implications in disease. *Febs J* 2021; 288(24): 7162-7182.
23. Lindner D, Zietsch C, Becher PM, et al. Differential expression of matrix metalloproteases in human fibroblasts with different origins. *Biochem Res Int* 2012; 2012(875742).
24. Baghirova S, Hughes BG, Poirier M, Kondo MY, Schulz R. Nuclear matrix metalloproteinase-2 in the cardiomyocyte and the ischemic-reperfused heart. *J Mol Cell Cardiol* 2016; 94(153-161).
25. Rodrigues M, Xin X, Jee K, et al. VEGF secreted by hypoxic Muller cells induces MMP-2 expression and activity in endothelial cells to promote retinal neovascularization in proliferative diabetic retinopathy. *Diabetes* 2013; 62(11): 3863-3873.
26. Xiang ZL, Zeng ZC, Fan J, Tang ZY, Zeng HY, Gao DM. Gene expression profiling of fixed tissues identified hypoxia-inducible factor-1alpha, VEGF, and matrix metalloproteinase-2 as biomarkers of lymph node metastasis in hepatocellular carcinoma. *Clin Cancer Res* 2011; 17(16): 5463-5472.
27. Liu W, Zhang W, Wang T, et al. Obstructive sleep apnea syndrome promotes the progression of aortic dissection via a ROS- HIF-1alpha-MMPs associated pathway. *Int J Biol Sci* 2019; 15(13): 2774-2782.
28. Gao CK, Liu H, Cui CJ, Liang ZG, Yao H, Tian Y. Roles of MicroRNA-195 in cardiomyocyte apoptosis induced by myocardial ischemia-reperfusion injury. *J Genet* 2016; 95(1): 99-108.
29. Yu SY, Dong B, Fang ZF, Hu XQ, Tang L, Zhou SH. Knockdown of lncRNA AK139328 alleviates myocardial ischaemia/reperfusion injury in diabetic mice via modulating miR-204-3p and inhibiting autophagy. *J Cell Mol Med* 2018; 22(10): 4886-4898.
30. Wang W, Schulze CJ, Suarez-Pinzon WL, Dyck JR, Sawicki G, Schulz R. Intracellular action of matrix metalloproteinase-2 accounts for acute myocardial ischemia and reperfusion injury. *Circulation* 2002; 106(12): 1543-1549.
31. Maarman G, Marais E, Lochner A, du Toit EF. Effect of chronic CPT-1 inhibition on myocardial ischemia-reperfusion injury (I/R) in a model of diet-induced obesity. *Cardiovasc Drug Ther* 2012; 26(3): 205-216.
32. Kaestner KH, Knochel W, Martinez DE. Unified nomenclature for the winged helix/forkhead transcription factors. *Gene Dev* 2000; 14(2): 142-146.
33. Wijchers PJ, Burbach JP, Smidt MP. In control of biology: of mice, men and Foxes. *Biochem J* 2006; 397(2): 233-246.
34. Eckle T, Kohler D, Lehmann R, El KK, Eltzschig HK. Hypoxia-inducible factor-1 is central to cardioprotection: a new paradigm for ischemic preconditioning. *Circulation* 2008; 118(2): 166-175.
35. Thomas LW, Ashcroft M. Exploring the molecular interface between hypoxia-inducible factor signalling and mitochondria. *Cell Mol Life Sci* 2019; 76(9): 1759-1777.
36. Dong J, Xu M, Zhang W, Che X. Effects of Sevoflurane Pretreatment on Myocardial Ischemia-Reperfusion Injury Through the Akt/Hypoxia-Inducible Factor 1-alpha (HIF-1alpha)/Vascular Endothelial Growth Factor (VEGF) Signaling Pathway. *Med Sci Monitor* 2019; 25(3100-3107).
37. Wang X, Ma S, Qi G. Effect of hypoxia-inducible factor 1-alpha on hypoxia/reoxygenation-induced apoptosis in primary neonatal rat cardiomyocytes. *Biochem Bioph Res Co* 2012; 417(4): 1227-1234.
38. Wang GY, Bergman MR, Nguyen AP, et al. Cardiac transgenic matrix metalloproteinase-2 expression directly induces impaired contractility. *Cardiovasc Res* 2006; 69(3): 688-696.
39. Bergman MR, Teerlink JR, Mahimkar R, et al. Cardiac matrix metalloproteinase-2 expression independently induces marked ventricular remodeling and systolic dysfunction. *Am J Physiol-Heart C* 2007; 292(4): H1847-H1860.
40. Ceron CS, Baligand C, Joshi S, et al. An intracellular matrix metalloproteinase-2 isoform induces tubular regulated necrosis: implications for acute kidney injury. *Am J Physiol-Renal* 2017; 312(6): F1166-F1183.
41. Ali MA, Cho WJ, Hudson B, Kassiri Z, Granzier H, Schulz R. Tintin is a target of matrix metalloproteinase-2: implications in myocardial ischemia/reperfusion injury. *Circulation* 2010; 122(20): 2039-2047.
42. Diao SL, Xu HP, Zhang B, Ma BX, Liu XL. Associations of MMP-2, BAX, and Bcl-2 mRNA and Protein Expressions with Development of Atrial Fibrillation. *Med Sci Monitor* 2016; 22(1497-1507).
43. Lin HB, Cadete VJ, Sra B, et al. Inhibition of MMP-2 expression with siRNA increases baseline cardiomyocyte contractility and protects against simulated ischemic reperfusion injury. *Biomed Res Int* 2014; 2014(810371).
44. Zhou T, Chuang CC, Zuo L. Molecular Characterization of Reactive Oxygen Species in Myocardial Ischemia-Reperfusion Injury. *Biomed Res Int* 2015; 2015(864946).
45. Stamenkovic A, O'Hara KA, Nelson DC, et al. Oxidized phosphatidylcholines trigger ferroptosis in cardiomyocytes during

- ischemia-reperfusion injury. *Am J Physiol-Heart C* 2021; 320(3): H1170-H1184.
46. Zhao WK, Zhou Y, Xu TT, Wu Q. Ferroptosis: Opportunities and Challenges in Myocardial Ischemia-Reperfusion Injury. *Oxid Med Cell Longev* 2021; 2021(9929687).
47. Li W, Li W, Leng Y, Xiong Y, Xia Z. Ferroptosis Is Involved in Diabetes Myocardial Ischemia/Reperfusion Injury Through Endoplasmic Reticulum Stress. *Dna Cell Biol* 2020; 39(2): 210-225.